



Article

Piezoresistive Response of Carbon Nanotube Yarn Monofilament Composites under Axial Compression

Iriana Garcia Guerra, Tannaz Tayyarian, Omar Rodríguez-Uicab and Jandro L. Abot *

Department of Mechanical Engineering, The Catholic University of America, Washington, DC 20064, USA

* Correspondence: abot@cua.edu

Abstract: The hierarchical structure and microscale dimensions of carbon nanotube yarns (CNTYs) make them great candidates for the development of integrated sensing applications. The change in the electrical resistance of CNTYs due to mechanical strain, known as piezoresistivity, is the principal mechanism in strain sensing using CNTYs. While the axial tensile properties of CNTYs have been studied widely, studies on the axial piezoresistive response of CNTYs under compression have been limited due to the complexities associated with the nature of the experiments involving subjecting a slender fiber to compression loading in its axial direction. In this study, the piezoresistive response of a single CNTY embedded into a polymeric resin (CNTY monofilament composite) was investigated under axial compression. The results suggest that the CNTY exhibits a strong piezoresistive response in the axial direction with sensitivity or gauge factor values in the order of 0.4–0.5 for CNTY monofilament composites. The piezoresistive response of the CNTY monofilament composites under compression was compared to that under tension and it was observed that the sensitivity appears to be slightly lower under compression. The potential change in sensitivity between the freestanding CNTY and the CNTY monofilament composite under compression is still unknown. Knowing the axial piezoresistive response of the CNTYs under both tension and compression will enable their use in sensing applications where the yarn undergoes compression including those in aerospace and marine structures, and civil or energy infrastructure.



Citation: Garcia Guerra, I.; Tayyarian, T.; Rodríguez-Uicab, O.; Abot, J.L. Piezoresistive Response of Carbon Nanotube Yarn Monofilament Composites under Axial Compression. *C* **2023**, *9*, 89. <https://doi.org/10.3390/c9040089>

Academic Editor: Patrizia Savi

Received: 3 March 2023

Revised: 29 August 2023

Accepted: 12 September 2023

Published: 25 September 2023



Copyright: © 2023 by the authors. Licensee MDPI, Basel, Switzerland. This article is an open access article distributed under the terms and conditions of the Creative Commons Attribution (CC BY) license (<https://creativecommons.org/licenses/by/4.0/>).

Keywords: carbon nanotube yarn; piezoresistive response; axial compression; monofilament composites; tension-compression

1. Introduction

Carbon nanotubes (CNTs) have been shown to exhibit extraordinary mechanical, electrical, and thermal properties [1]. Since their discovery in 1991, there has been great interest in tapping into their sensing capabilities for a variety of applications. In order to be utilized as piezoresistive sensors for strain monitoring, CNTs could be in the form of just nanotubes [2], sheets and thin films [3,4], or fibers and yarns [5–12]. Carbon nanotube yarns (CNTYs) are continuous fiber-like materials consisting of thousands of individual CNTs in their cross-section that can be twisted and densified to form a yarn, and further tailored to serve as in situ sensors in structural health monitoring (SHM) due to their significant sensitivity to strain, small size, light weight, high surface area, high electrical and thermal conductivity, and multifunctionality [12–14]. Some studies show that CNTYs exhibit an elastic modulus ranging from 70 to 350 GPa and a tensile strength ranging from 0.23 to 8.8 GPa [1,15]. Thus, the elastic modulus of CNTY can be greater than that of aluminum (70 GPa) and of steel (210 GPa). Moreover, recent studies also show that the specific electrical conductivity of CNTYs may reach a maximum of $19.6 \times 10^6 \text{ Sm}^{-1}\text{g}^{-1}\text{cm}^3$ exceeding $14.15 \times 10^6 \text{ Sm}^{-1}\text{g}^{-1}\text{cm}^3$ and $6.52 \times 10^6 \text{ Sm}^{-1}\text{g}^{-1}\text{cm}^3$, which correspond to the specific electrical conductivity of aluminum and copper, respectively [16]. However, one of the most relevant properties of the CNTY for sensing is piezoresistivity, which causes the electrical resistance to change when a mechanical strain is applied [8–10]. From

a nanoscale perspective, for low tensile strain levels (<2%), metallic nanotubes play a paramount role in the change of electrical resistance [17]. For high tensile strain levels, above 5%, semiconducting nanotubes dominate the change in the electrical resistance of the CNTYs [17]. There are two underlying phenomena that take place at different strain rates [18]. It is said that the bundles of carbon nanotubes untwist during tensile loading and their contact length decreases (the density of CNTYs per unit length decreases), which leads to an increase in electrical resistance [19]. In contrast, the electrical resistance decreases during the unloading segments [17–19]. In addition, there is a decrease in electrical resistance that occurs due to inter-tube/inter-bundle slippage (inelastic shear motion) caused by the yarn's relaxation and structural reformation during the loading segments, and a continuous decrease in electrical resistance occurs during unloading as the yarn recovers its (conductive) structure [19]. Based on previous studies, the first phenomenon, whereby an electrical resistance increase is recorded during the loading and a decrease in electrical resistance in the unloading segments is dominant at high tensile strain rates. At a very low quasi-static tensile strain rate, an electrical resistance decrease during both loading and unloading segments has been reported [18–23]. In this study, the axial piezoresistive response of the CNTY monofilament composites was investigated under compression for a variety of strain rates and the results were compared with those of the piezoresistive response of CNTY monofilament composites under tension.

2. Materials, Fabrication and Characterization

2.1. Materials

The CNTY used in this study was fabricated from a vertically aligned CNT array at Nanoworld Laboratories (Cincinnati, OH, USA). The diameter, density, angle of twist, and average electrical resistivity of the densified CNTYs are $\sim 30 \mu\text{m}$, $\sim 0.65 \text{ g/cm}^3$, $\sim 30^\circ$, and $1.7 \times 10^{-3} \Omega \text{ cm}$, respectively [19–23]. The corresponding electrical conductivity value is about $3.337 \times 10^{-5} \text{ S/m}$. Figure 1 shows images of the twisted yarn obtained by Scanning Electron Microscopy (SEM). Figure 1a shows an image of the CNTY with a magnification of $5000\times$ and Figure 1b shows an image with a magnification of $50,000\times$.

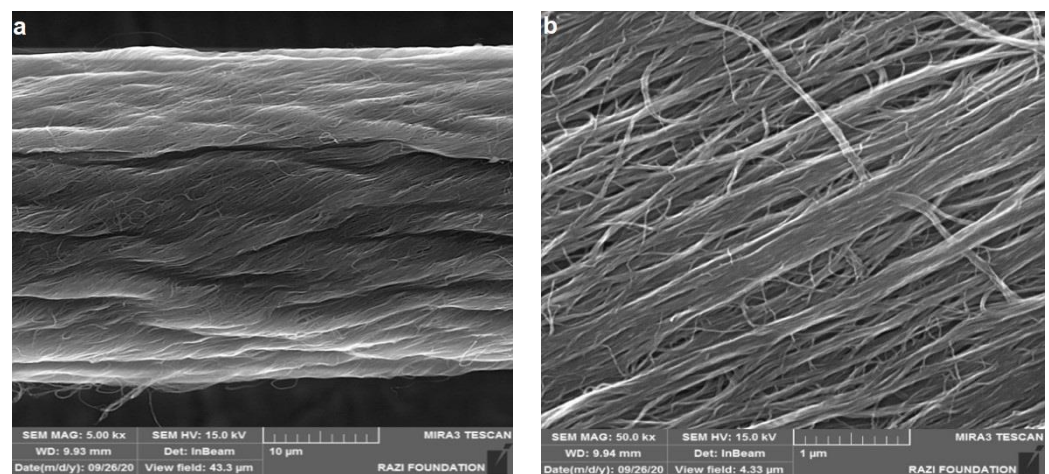


Figure 1. Scanning Electron Microscopy images of CNTY: (a) $5000\times$; (b) $50,000\times$ (images were taken by MIRA3 TESCAN).

A commercial thermosetting epoxy resin, Epon 862 (Diglycidyl Ether of Bisphenol F) and Epikure W (aromatic amine) curing agent, both from Miller-Stephenson Chemical Co. (Danbury, CT, USA), was used as the polymeric matrix of the CNTY monofilament composites.

2.2. Fabrication

A schematic of the CNTY monofilament composite sample is shown in Figure 2. A CNTY is embedded into a polymer to form a CNTY monofilament composite using a silicon rubber mold. Four 40 AWG copper wire electrodes were parallelly incorporated into the silicone mold. The wires were threaded through needles and then stitched through the mold at the pre-marked positions at the mid-thickness (5 mm from the surface) and mid-length of the mold. The wires were positioned under the CNTY to eliminate any stress caused by the contact between the wires and the CNTY. The next step consisted of integrating the CNTY into the mold. The CNTY was removed gently from the spool and placed so that its length exceeded the length of the rubber mold, and it was prestressed with a small weight to ensure CNTY straightness of all the specimens. A conductive paint, Bare Paint™ (Bare Conductive, London, UK), was used to promote the ohmic contact between the CNTY and the copper wires. The dimensions of the specimen are based on the ASTM standard D695, which is recommended for characterizing mechanical properties of rigid polymers.

With a mixing ratio of 100:23 of resin and hardener, EPON 862 was mixed with Epikure W, and mixed in a beaker for 3 min. The mixture was heated to 130 °C for 15 min to eliminate air bubbles. Once the CNTY was straight and in place, previously mixed polymer was poured into the mold and it was inserted into a convection drying oven (Labnique, Hunt Valley, MD, USA) for curing. The specimens were cured using two-step heating cycles. During the first 2 h, the temperature was set to 100 °C and increased to 130 °C for the last 2 h of the heating cycle. The resulting specimens were 25.4 mm long, 12.7 mm wide, and 12.7 mm thick. Strain gauges were mounted on each side of the specimen as shown in Figure 2.

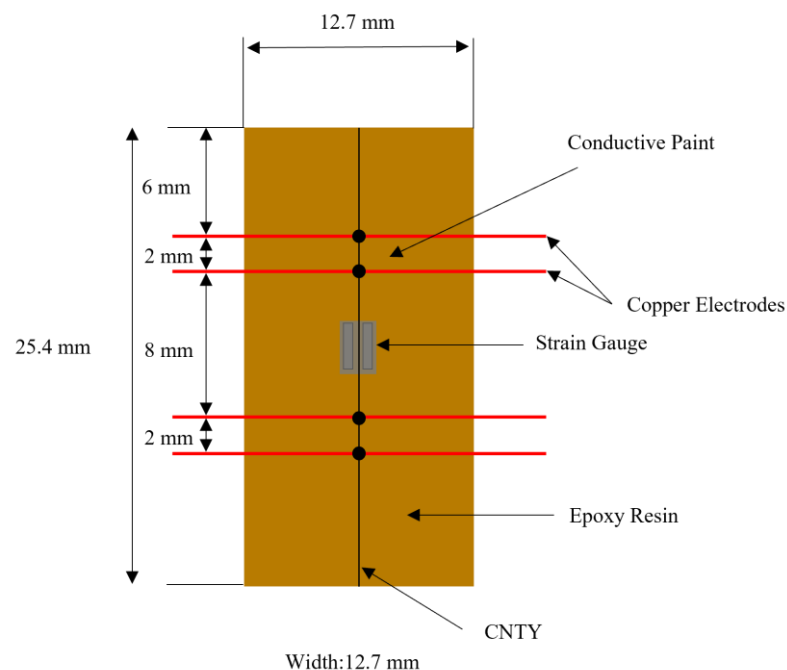


Figure 2. Schematic view of the CNTY monofilament composite specimen instrumented with strain gauge.

2.3. Electrical and Mechanical Measurements

A MTS Criterion 43 electromechanical loading machine with a 30-kN capacity load cell, controlled by the TestWorks4 software, was used to apply the load to the specimens at various strain rates for at least five continuous compression cyclic loadings. All experiments were performed within the linear elastic regime of the polymeric material. The electrical resistance of the embedded CNTY was measured during the experiments using a four-

point-probe measurement technique with an NI PXI-4072 (Austin, TX, USA) Inductance–Capacitance–Resistance (LCR) card mounted in an NI PXI-1033 chassis. The four copper wires were inserted inside the specimen and connected to the NI-PXI-4072 card using Bayonet Neill–Concelman (BNC) cables and electrical leads with mini-hooks. The electrical resistance (R) of the embedded CNTY was determined by using inner probes that measure the voltage (V) while a constant current (I) was applied using the outer probes. The strain was measured by connecting the strain gauges (attached to the mid-center of the specimen) to an NI-PXI 9219 card mounted on an NI cDAQ-9178 chassis. The experimental setup is shown in Figure 3. The applied load, strain, and electrical resistance were measured as a function of time. The data acquisition was conducted at 2 Hz using NI SignalExpress 2015 software. Five specimens of CNTY monofilament composite materials for each experiment were tested to ensure reproducibility.

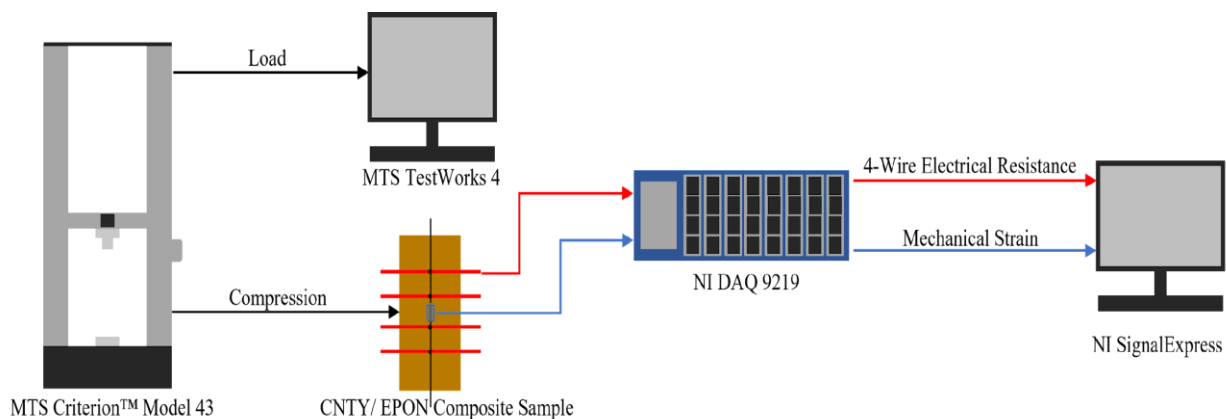


Figure 3. Schematic of experimental setup for mechanical and electrical measurements.

2.4. Scanning Electron Microscopy

The fracture surface morphology of the CNTY monofilament composite specimens was investigated to study the effect of wetting, wicking, and resin infiltration into the porous structure of the yarn. The fracture surface of CNTY monofilament composite specimens was examined by Scanning Electron Microscopy (SEM). SEM was conducted using a FEG-SEM field-emission MIRA3 TESCAN SEM (Kohoutovice, Czech Republic) operated at an acceleration voltage (ACC V) of 15 kV. The specimens were cross-sectionally cut by means of liquid nitrogen and their cross-sectional area was coated with a thin layer of gold using the Quorum Q150R ES–magnetron sputtering machine (Laughton, East Sussex, UK).

3. Results and Discussion

3.1. Piezoresistive Response of CNTY Monofilament Composites under Uniaxial Compression

The electrical resistance of the embedded CNTY and the strain were simultaneously measured throughout the experiments. The relative electrical resistance change ($\Delta R/R_0$) and strain (ϵ) versus time responses of the CNTY monofilament composites subjected to ten continuous compression cycles at a constant strain rate of 0.04 min^{-1} are shown in Figure 4. The strain (ϵ) experienced by the specimen is shown at the right vertical axis (red) while the relative change in electrical resistance ($\Delta R/R_0$) is shown at the left vertical axis (black), both plotted as a function of time. It is shown that both ϵ and $\Delta R/R_0$ decreased during loading and increased during unloading segments, thus indicating a positive piezoresistive response. The data show good repeatability, linearity, and consistency in the peak locations and values of $\Delta R/R_0$ and ϵ at each cycle. The maximum strain reaches -0.36% when the compressive load reaches $\sim 2000 \text{ N}$, which is equivalent to a compressive stress of 12.4 MPa , and returns to 0 at the end of the unloading segment, while $\Delta R/R_0$ reaches -0.15% and returns to 0 upon unloading. It is worth mentioning that this stress level is well within the linear elastic regime of the mechanical response of the polymeric matrix of the monofilament composite.

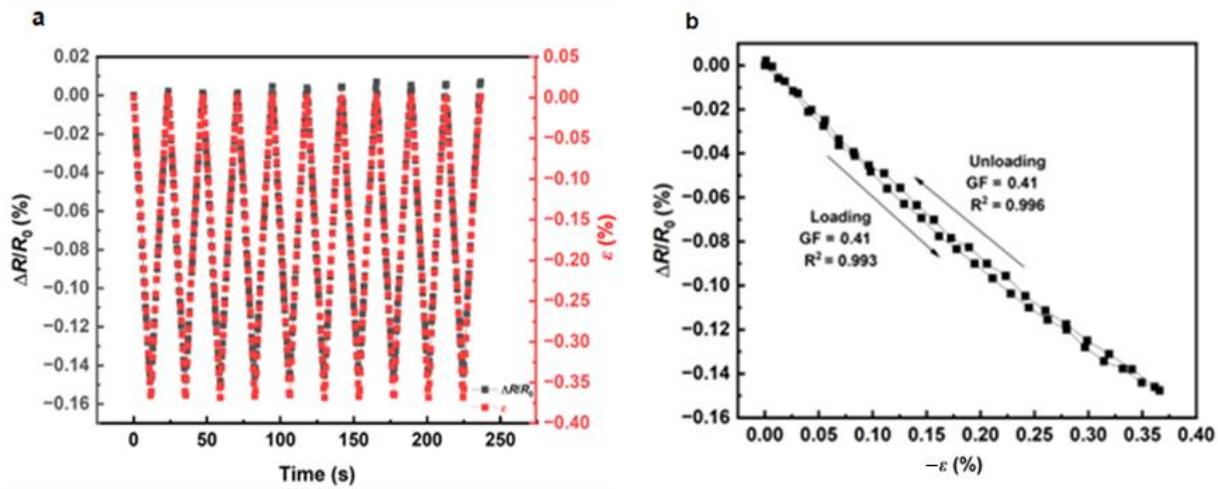


Figure 4. CNTY monofilament composite under axial compression at a strain rate of 0.04 min^{-1} : (a) Relative change of electrical resistance and strain versus time; (b) Relative change of electrical resistance versus strain.

The $\Delta R/R_0$ versus ϵ curves showing one cycle (loading-unloading) up to a maximum strain of -0.36% are presented in Figure 4. It shows that the CNTY monofilament composite exhibits a quasi-linear positive piezoresistive response under compressive loading and unloading segments up to this strain level.

The sensitivity or gauge factor (GF) of the piezoresistive response of the CNTY monofilament composite is defined as the slope of the relative change of electrical resistance versus strain and can be calculated according to:

$$GF = \frac{\frac{\Delta R}{R_0}}{\epsilon} \quad (1)$$

A positive GF of 0.41 ± 0.01 was recorded for the CNTY monofilament composites under compressive loading considering the loading segment of one of the cycles. Similar results were obtained for the unloading segments.

3.1.1. Strain Rate Effect

Based on previous studies that had shown a significant effect of the strain rate on the piezoresistive response of freestanding CNTYs under tension [16], a similar study was pursued to determine the effect of the strain rate on the piezoresistive response of the CNTY monofilament composites under axial compression. The specimens were subjected to compressive cycles at other strain rates, including 0.02 min^{-1} , 0.2 min^{-1} , 0.4 min^{-1} , and 0.6 min^{-1} . The relative resistance change ($\Delta R/R_0$) and strain (ϵ) versus time responses of the CNTY monofilament composites at these four different strain rates are shown in Figure 5a–d. The compressive strain (ϵ) experienced by the specimen is plotted at the right vertical axis (red) while the relative change in electrical resistance ($\Delta R/R_0$) is shown at the left vertical axis (black), both plotted as a function of time.

The results showed that for all strain rates, there was a decrease in $\Delta R/R_0$ during loading and an increase during unloading. At a strain rate of 0.02 min^{-1} , the maximum strain was $-0.36 \pm 0.01\%$, and $\Delta R/R_0$ was -0.14% . For a strain rate of 0.2 min^{-1} , the maximum strain was also $-0.36 \pm 0.01\%$, and $\Delta R/R_0$ was -0.15% . At a strain rate of 0.4 min^{-1} , the maximum strain was $-0.32 \pm 0.02\%$, and $\Delta R/R_0$ was -0.13% . Finally, at a strain rate of 0.6 min^{-1} , the maximum strain was $-0.30 \pm 0.02\%$, and $\Delta R/R_0$ was -0.12% . In all cases, the maximum strain was reached when the compressive load was 2000 N (12.4 MPa), and it returned to 0 at the end of the unloading segment.

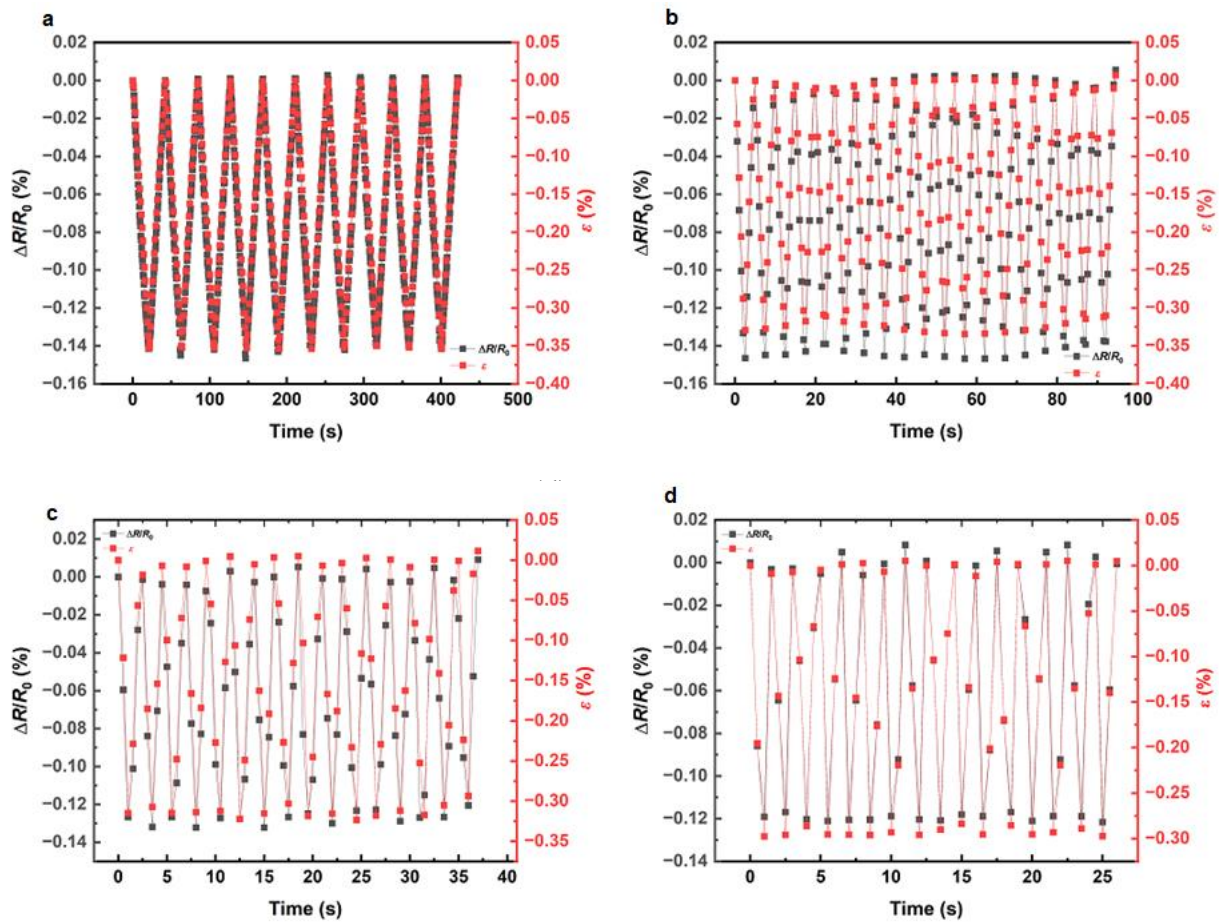


Figure 5. Relative change of electrical resistance and strain versus time of CNTY monofilament composites under axial compression at strain rates of: (a) 0.02 min^{-1} ; (b) 0.2 min^{-1} ; (c) 0.4 min^{-1} ; (d) 0.6 min^{-1} . In each instance, the maximum compressive load reached 2000 N (stress of 12.4 MPa) and reached 0 at the conclusion of the unloading period.

Figure 6a–d shows the piezoresistive response of the CNTY monofilament composite specimens during a compressive loading–unloading cycle for the same strain rates, including 0.02 min^{-1} , 0.2 min^{-1} , 0.4 min^{-1} , and 0.6 min^{-1} . For all strain rates, the piezoresistive response is quasi-linear for both loading and unloading segments, and some hysteresis was observed, being more prominent at the higher rates. As observed for the strain rate of 0.04 min^{-1} , the data show good repeatability, linearity, and consistency in the peak locations and values of $\Delta R/R_0$ and ϵ at each cycle.

Table 1 summarizes the sensitivity (gauge factor, GF) for the five different strain rates, including the corresponding maximum strain level and maximum relative change in electrical resistance. It is concluded that the sensitivity varies slightly with increasing strain rate.

Table 1. Sensitivity of CNTY monofilament composites under axial compression for various strain rates.

Strain Rate $-\dot{\epsilon} \text{ (min}^{-1}\text{)}$	Strain Level $-\epsilon \text{ (%)}$	Relative Change in Electrical Resistance $\Delta R/R_0 \text{ (%)}$	GF
0.02	0.36	−0.14	0.41 ± 0.01
0.04	0.36	−0.15	0.41 ± 0.01
0.2	0.33	−0.15	0.45 ± 0.01
0.4	0.32	−0.13	0.41 ± 0.01
0.6	0.30	−0.12	0.41 ± 0.01

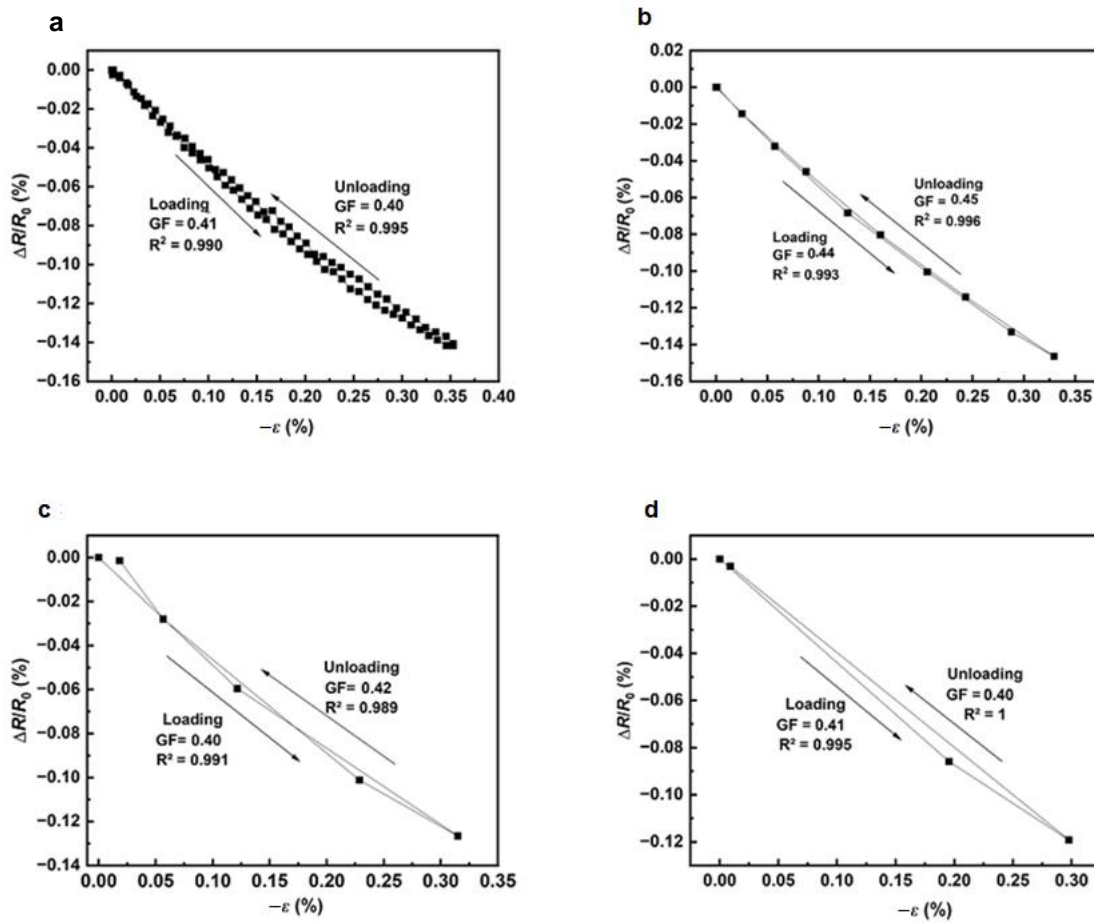


Figure 6. Relative change of resistance-strain of CNTY monofilament composites under loading-unloading cycles at strain rates of: (a) 0.02 min^{-1} ; (b) 0.2 min^{-1} ; (c) 0.4 min^{-1} ; (d) 0.6 min^{-1} .

3.1.2. Hysteresis

The hysteresis of the piezoresistive response of the CNTY monofilament composites was quantified using two parameters: the residual relative change in electrical resistance $(\Delta R/R_0)_{\text{Res}}$, which is defined as the difference between the initial and final values of $\Delta R/R_0$ after each cycle, and a path-dependent metric (H), which is defined as the area between the loading-unloading curve at each cycle. H is dependent on the maximum relative change in resistance $(\Delta R/R_0)_{\text{max}}$ and the maximum strain change $(\epsilon)_{\text{max}}$ during the loading phase of each cycle. Figure 7 shows the schematic of the parameters calculated after each cycle. The normalized hysteresis (H_N) is defined as:

$$H_N = \frac{H}{\left(\frac{\Delta R}{R_0}\right)_{\text{max}} (\epsilon)_{\text{max}}}$$

where H_N is the normalized hysteresis, H is the area under the hysteresis loop, $(\epsilon)_{\text{max}}$ represents the maximum strain achieved in each cycle, and $(\Delta R/R_0)_{\text{max}}$ is the maximum change in electrical resistance associated with the strain. Table 2 shows the corresponding values of the calculated hysteresis parameters for each strain rate tested.

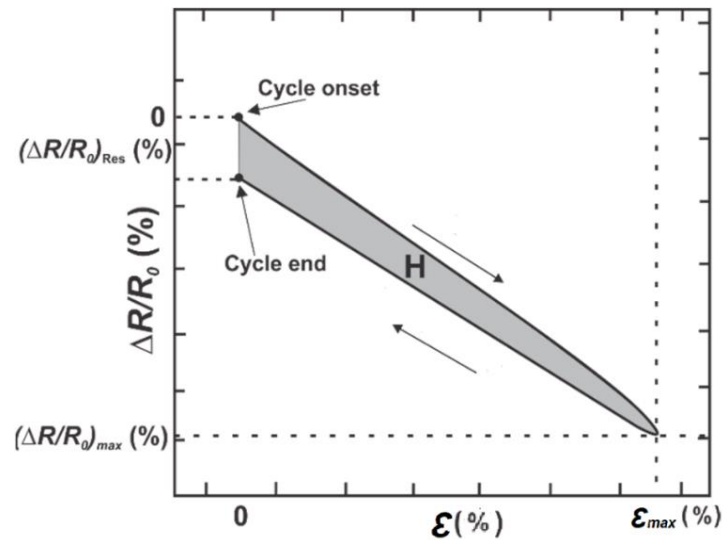


Figure 7. Schematic of the experimental parameters used for piezoresistive analysis.

Table 2. Hysteresis parameters of CNTY monofilament composites under axial compression for various strain rates.

Strain Rate $-\dot{\epsilon}$	Hysteresis H_N (%)
0.04	-0.031 ± 0.010
0.02	-0.024 ± 0.022
0.2	-0.010 ± 0.017
0.4	-0.0027 ± 0.015
0.6	-0.035 ± 0.011

3.1.3. Stress-Strain Response

When subjected to compressive forces up to 2000 N, the stress-strain behavior of the monofilament composite follows a linear curve (Figure 8). This linear behavior indicates that the material undergoes elastic deformation. The linear portion of the stress-strain curve can be characterized by the elastic modulus (approximately 3.7 GPa). The linear stress-strain behavior of the CNTY monofilament composite can be explained by the strong bonding between the CNTYs and the polymeric matrix. Under compressive forces, the CNTYs transmit the load to the polymer matrix through interfacial shear stresses. The interfacial shear stresses are proportional to the deformation, resulting in a linear stress-strain curve. The linear behavior can be maintained until the CNTs start to buckle or the polymer matrix undergoes plastic deformation. Increasing the stress level leads to nonlinearity, which would correspond to the nonlinearity of the polymer itself as well as that of the CNTY.

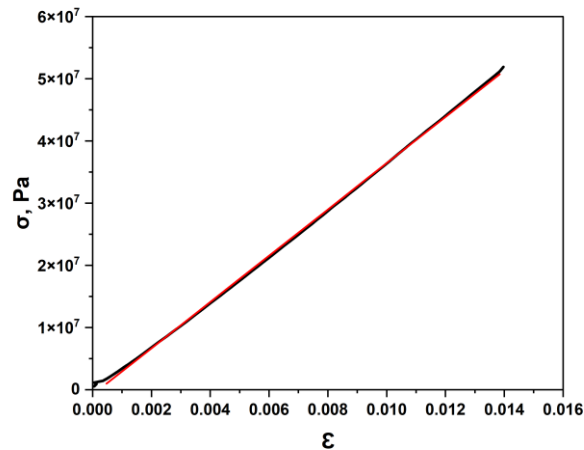


Figure 8. Stress-strain curve of CNTY monofilament composite under compressive loading cycle (second cycle).

3.2. Scanning Electron Microscopy

Figure 9a,b show the fracture surface SEM images of CNTY embedded in the monofilament composite. The images show that only the outer bundles are affected by resin infiltration and show no evidence of fiber/matrix debonding. The images indicate that the piezoresistive response of the embedded yarn could be predominantly dependent on the change of the contact resistance between the internal bundles upon deformation because the resin exhibits relatively conservative infiltration into the yarn, consequently exerting a comparatively minor influence during strain.

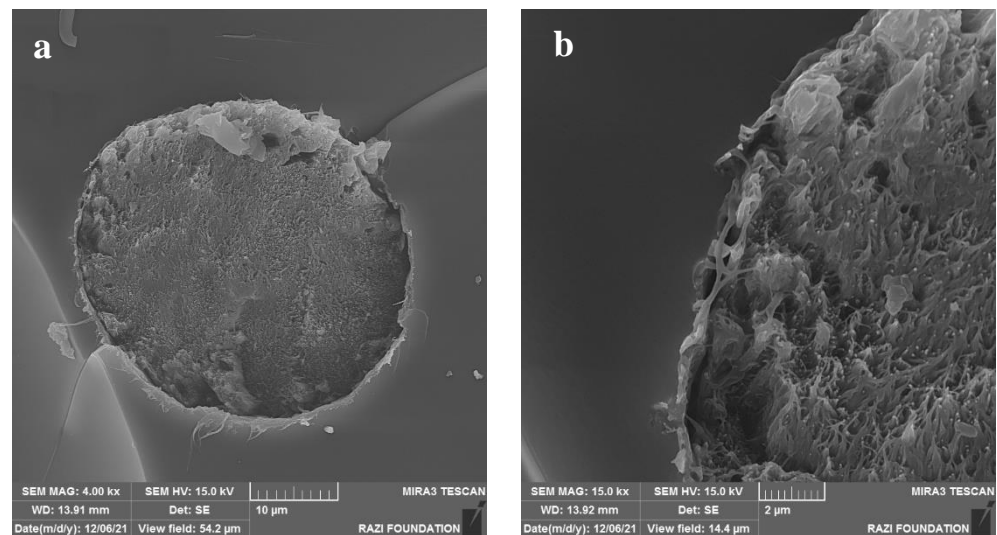


Figure 9. Scanning Electron Microscopy (SEM) images of the CNTY monofilament composite cross-section at: (a) 4000 \times ; (b) 15,000 \times (images were taken by MIRA3 TESCAN) [24].

3.3. Comparison of Piezoresistive Responses of Monofilament Composites under Uniaxial Compression and Tension

The piezoresistive response of the CNTY monofilament composite under uniaxial longitudinal compression was compared to prior and new results on the piezoresistive response of the CNTY monofilament composite under tension.

These results appear to indicate that the piezoresistive responses of the CNTY monofilament composite under tension and compression are substantially similar. For instance, Figure 10 shows there is an overlap between the relative electrical resistance change ($\Delta R/R_0$) and strain (ϵ) versus time responses of the CNTY monofilament composites subjected to

nine continuous tension cycles at a constant strain rate of 0.01 min^{-1} and 0.05 min^{-1} , respectively.

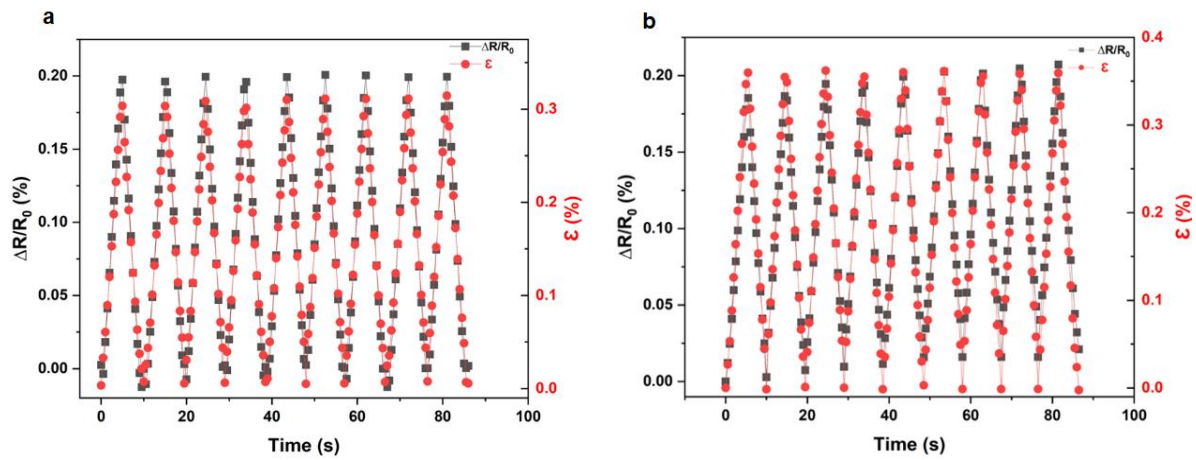


Figure 10. Relative change of electrical resistance and strain versus time of CNTY monofilament composite under axial tension at a strain rate: (a) 0.01 min^{-1} ; (b) 0.05 min^{-1} .

The strain (ϵ) experienced by the specimen is shown at the right vertical axis (red) while the relative change in electrical resistance ($\Delta R/R_0$) is shown at the left vertical axis (black), both plotted as a function of time. It is shown that both ϵ and $\Delta R/R_0$ increased during loading and decreased during unloading segments, thus indicating a positive piezoresistive response. The data show good repeatability, linearity, and consistency in the peak locations and values of $\Delta R/R_0$ and ϵ at each cycle. The maximum strain reaches 0.36% and 0.32% when the tensile load reaches 500 N and returns to 0 at the end of the unloading segment, while $\Delta R/R_0$ reaches 0.20% and returns to 0 upon unloading. Similar to the compression studies, the consistent correspondence between strain and electrical resistance change over multiple cycles indicates a predictable piezoresistive response of the CNTY. This predictability underscores the potential of the CNTY monofilament composite as a reliable and repeatable piezoresistive sensor. Such sensors can find applications in structural health monitoring, fatigue assessment, and stress analysis, where precise and repetitive strain measurements are essential.

Another resemblance can be observed through the $\Delta R/R_0$ versus ϵ curve, where the CNTY monofilament composite exhibits a quasi-linear positive piezoresistive response under tension. Figure 11 presents the $\Delta R/R_0$ versus ϵ curves showing one cycle (loading-unloading) up to the maximum strain. Additionally, it is noteworthy that the gauge factor obtained, 0.53, closely resembles the gauge factor acquired during compression testing.

These results appear to indicate that the piezoresistive response of the CNTY monofilament composite under tension and compression are of the same order of magnitude, but more parametric studies are needed. The results also differ quite significantly from those of the freestanding CNTYs under axial tension, where the strain rate plays a very significant role in determining the sign of the piezoresistivity and the sensitivity. It is worth mentioning one more time that the piezoresistive response of the freestanding CNTY under compression is not available, due to the complexities associated with testing a very slender fiber under axial compression.

Different mechanisms are involved in the electrical response of the CNTY monofilament composite (embedded or constrained CNTY). Under tension, the contact resistance between the individual CNTs and their bundles is the main component governing the change in the electrical resistance of the CNTY. Assuming that, under tension, the contact area between individual CNTs and their bundles decreases due to the discrete length of nanotubes in the yarn, this results in a higher change in the electrical resistance under tension. Another contributing factor in the piezoresistive response of the CNTY monofilament composite is the effect of slippage. CNTY has a porous structure that promotes resin

infiltration. However, the high viscosity and high molecular weight of the polymeric matrix prevents infiltration. Therefore, fiber slippage and unravelling during tension could also be attributed to the higher piezoresistive response of the CNTY monofilament composites under tension.

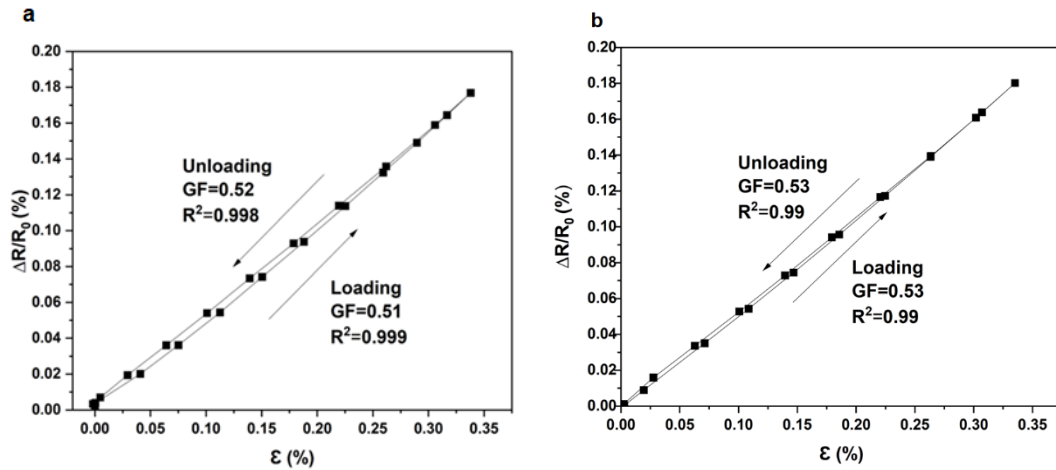


Figure 11. Relative change of electrical resistance versus strain of CNTY monofilament composites under loading-unloading cycle (fifth cycle) at strain rate: (a) 0.01 min^{-1} ; (b) 0.05 min^{-1} .

It is assumed that the cross-sectional volume of individual CNTs and their bundles increases when the CNTY monofilament composite is subjected to axial compression. By increasing the volume of the individual CNTs, the contact area between the CNTs and their bundle increases, which reduces the electrical resistance. However, despite the porous structure of the yarn, the distance between nanotubes is less affected under compression. As seen in Figure 9, CNTs and bundles are closely packed in the cross-sectional area of the embedded yarn. It is assumed that the increase in the cross-sectional volume of CNTs and their bundles, elimination of slippage, and fiber unravelling under compression are the main contributing phenomena to the piezoresistive response of the embedded yarn under compression.

4. Conclusions

The piezoresistive response of CNTY monofilament composites was investigated under axial compression. The aim was to understand the compressive piezoresistive response of the CNTYs for their implementation as piezoresistive-based sensors. This was done by embedding a single CNTY into a polymer to form a CNTY monofilament composite and subjecting it to axial compressive loading while monitoring the change in electrical resistance of the CNTY. In order to investigate the piezoresistive response, the CNTY monofilament composites were subjected to continuous compression cycles. The specimens were subjected to different quasi-static strain rates to study the effect of strain rate on the piezoresistive response of the CNTY. The relative change in electrical resistance of the CNTY monofilament composite decreases monotonically with the compressive strain and increases upon unloading. A positive piezoresistive response was observed for all strain rates with an excellent matching between the mechanical and electrical response cycles. The sensitivity of the CNTY monofilament composite, defined as the slope of the relative change of the electrical resistance over strain, was recorded during the loading and unloading compression segments. The sensitivity ranged from 0.4 to 0.45, considering a maximum strain level of approximately 0.35%. It was shown that the strain rate plays a relatively small role on the piezoresistive response of the embedded CNTY. Knowing the axial piezoresistive response of the CNTYs under both tension and compression will enable their use in sensing applications where the yarn undergoes compression, including those in aerospace and marine structures, and civil or energy infrastructure.

Author Contributions: I.G.G. was the student who conducted most of the work. I.G.G., T.T., O.R.-U. and J.L.A. wrote the first version of the paper. J.L.A. provided the main idea. I.G.G. and T.T. analyzed the data and wrote the paper. J.L.A. provided the laboratory facilities, expertise, technical input and reviewed the final write-ups along with O.R.-U. All authors have read and agreed to the published version of the manuscript.

Funding: This research was supported by the National Aeronautics Space Administration (NASA) District of Columbia Space Grant Consortium (DCSGC) with grants NNX15AT64H S11 and NNX15AT64H S12 and 80NSSC20M0092 to Jandro L. Abot.

Data Availability Statement: The data presented in this study are available on request from the corresponding author. The data are not publicly available due to privacy concerns.

Acknowledgments: The authors would like to thank the Department of Mechanical Engineering at The Catholic University of America. The authors acknowledge the financial support from the National Aeronautics and Space Administration (NASA) District of Columbia Space Grant Consortium (DCSGC). The authors would also like to thank Maria Erquiaga and Cagney Boyle for fabricating many of the specimens used in the experiments.

Conflicts of Interest: The authors declare no conflict of interest.

References

1. Abot, J.L.; Rajan, C.P. Carbon nanotube fibers. In *Carbon Nanomaterials Sourcebook: Graphene, Fullerenes, Nanotubes, and Nanodiamonds*; Sattler, K.D., Ed.; Taylor and Francis: London, UK, 2016; Volume I, pp. 357–383.
2. Thostenson, E.T.; Chou, T.-W. Real-time in situ sensing of damage evolution in advanced fiber composites using carbon nanotube networks. *Nanotechnology* **2008**, *19*, 215713. [[CrossRef](#)] [[PubMed](#)]
3. Obitayo, W.; Liu, T. A review: Carbon nanotube-based piezoresistive strain sensors. *J. Sens.* **2012**, *2012*, 652438. [[CrossRef](#)]
4. Wang, S.; Tang, L.A.; Bao, Q.; Lin, M.; Deng, S.; Goh, B.M.; Loh, K.P. Room temperature synthesis of soluble carbon nanotubes by the sonication of graphene oxide nanosheets. *J. Am. Chem. Soc.* **2009**, *131*, 16832–16837. [[CrossRef](#)] [[PubMed](#)]
5. Gspann, T.S.; Montinaro, N.; Pantano, A.; Elliott, J.A.; Windle, A.H. Mechanical properties of carbon nanotube fibres: St Venant's principle at the limit and the role of imperfections. *C* **2015**, *93*, 1021–1033. [[CrossRef](#)]
6. Zhao, J.; Zhang, X.; Pan, Z.; Li, Q. Wide-range tunable dynamic property of carbon-nanotube-based fibers. *Adv. Mater. Interfaces* **2015**, *2*, 1500093. [[CrossRef](#)]
7. Niu, M.; Cui, C.; Tian, R.; Zhao, Y.; Miao, L.; Hao, W.; Li, J.; Sui, C.; He, X.; Wang, C. Mechanical and thermal properties of carbon nanotubes in carbon nanotube fibers under tension–torsion loading. *RSC Adv.* **2022**, *12*, 30085–30093. [[CrossRef](#)]
8. Li, Y.-L.; Kinloch, I.A.; Windle, A.H. Direct spinning of carbon nanotube fibers from chemical vapor deposition synthesis. *Science* **2004**, *304*, 276–278. [[CrossRef](#)]
9. Alexopoulos, N.D.; Bartholome, C.; Poulin, P.; Marioli-Riga, Z. Structural health monitoring of glass fiber reinforced composites using embedded carbon nanotube (CNT) fibers. *Compos. Sci. Technol.* **2010**, *70*, 260–271. [[CrossRef](#)]
10. Wang, X.; Bradford, P.D.; Liu, W.; Zhao, H.; Inoue, Y.; Maria, J.-P.; Li, Q.; Yuan, F.-G.; Zhu, Y. Mechanical and electrical property improvement in CNT/nylon composites through drawing and stretching. *Compos. Sci. Technol.* **2011**, *71*, 1677–1683. [[CrossRef](#)]
11. Kahng, S.K.; Gates, T.S.; Jefferson, G.D. Strain and temperature sensing properties of multiwalled carbon nanotube yarn composites. In Proceedings of the SAMPE '08 Fall Technical Conference, Memphis, TN, USA, 8–10 September 2008.
12. Abot, J.L.; Schulz, M.J.; Song, Y.; Medikonda, S.; Rooy, N. Novel distributed strain sensing in polymeric materials. *Smart Mater. Struct.* **2010**, *19*, 085007. [[CrossRef](#)]
13. Abot, J.L.; Song, Y.; Vatsavaya, M.S.; Medikonda, S.; Kier, Z.; Jayasinghe, C.; Rooy, N.; Shanov, V.N.; Schulz, M.J. Delamination detection with carbon nanotube thread in self-sensing composite materials. *Compos. Sci. Technol.* **2010**, *70*, 1113–1119. [[CrossRef](#)]
14. Zhao, H.; Zhang, Y.; Bradford, P.D.; Zhou, Q.; Jia, Q.; Yuan, F.; Zhu, Y. Carbon nanotube yarn strain sensors. *Nanotechnology* **2010**, *21*, 305502. [[CrossRef](#)]
15. Zhao, J.; Zhang, X.; Di, J.; Xu, G.; Yang, X.; Liu, X.; Yong, Z.; Chen, M.; Li, Q. Double-peak mechanical properties of carbon-nanotube fibers. *Small* **2010**, *6*, 2612–2617. [[CrossRef](#)] [[PubMed](#)]
16. Zhao, Y.; Wei, J.; Vajtai, R.; Ajayan, P.M.; Barrera, E.V. Iodine doped carbon nanotube cables exceeding specific electrical conductivity of metals. *Sci. Rep.* **2011**, *1*, 83. [[CrossRef](#)] [[PubMed](#)]
17. Abot, J.L.; Alesh, T.; Belay, K. Strain dependence of electrical resistance in carbon nanotubes. *Carbon* **2014**, *70*, 95–112. [[CrossRef](#)]
18. Anike, J.; Bajar, A.; Abot, J.L. Time-dependent effects on the coupled mechanical-electrical response of carbon nanotube yarns under tensile loading. *C* **2016**, *2*, 3. [[CrossRef](#)]
19. Anike, J.; Le, H.H.; Brodeur, G.; Kadavan, M.; Abot, J.L. Piezoresistive response of integrated CNT yarns under compression and tension: The effect of lateral constraint. *C* **2017**, *3*, 14. [[CrossRef](#)]
20. Anike, J.C.; Belay, K.; Abot, J.L. Piezoresistive response of carbon nanotube yarns under tension: Parametric effects and phenomenology. *New Carbon Mater.* **2018**, *33*, 140–154. [[CrossRef](#)]

21. Anike, J.C.; Belay, K.; Abot, J.L. Effect of twist on the electromechanical properties of carbon nanotube yarns. *Carbon* **2019**, *142*, 491–503. [[CrossRef](#)]
22. Schadler, L.S.; Giannaris, S.C.; Ajayan, P.M. Load transfer in carbon nanotube epoxy composites. *Appl. Phys. Lett.* **1998**, *73*, 3842–3844. [[CrossRef](#)].
23. Lekawa-Raus, A.; Koziol, K.K.K.; Windle, A.H. Piezoresistive effect in carbon nanotube fibers. *ACS Nano* **2014**, *8*, 11214. [[CrossRef](#)].
24. Rodriguez-Uicab, O.; Tayyarian, T.; Abot, J.L. Effect of curing temperature of epoxy matrix on the electrical response of carbon nanotube yarn monofilament composites. *J. Compos. Sci.* **2022**, *6*, 43. [[CrossRef](#)]

Disclaimer/Publisher’s Note: The statements, opinions and data contained in all publications are solely those of the individual author(s) and contributor(s) and not of MDPI and/or the editor(s). MDPI and/or the editor(s) disclaim responsibility for any injury to people or property resulting from any ideas, methods, instructions or products referred to in the content.